

$\Gamma - X$ Resonant Tunneling Effect in AlAs/GaAs Single Quantum Barriers under Hydrostatic Pressure

Y. Carbonneau and J. Beerens

*Département de Physique, Université de Sherbrooke
Sherbrooke Québec J1K2R1, Canada*

L. A. Cury

*Departamento de Física, Universidade Federal de Minas Gerais
C.P. 702 30161-970 Belo Horizonte, MG, Brasil*

H. C. Liu and M. Buchanan

*Institut for Microstructural Sciences, National Research Council of Canada
Ottawa K1A0R6, Canada*

Received August 27; revised manuscript received September 20, 1993

We present an experimental study of intervalley transport in an AlAs/GaAs single quantum barrier at different hydrostatic pressures in the liquid helium temperature. Complementary studies at atmospheric pressure and different temperatures are also performed. Two regions of negative differential conductivity are observed in the current-voltage characteristics at all pressure and temperature ranges used. They are attributed to the resonant tunneling of Γ incident electrons through the X-valley levels in the AlAs barrier. Our experimental results are analysed within the effective mass approximation taking into account the $\Gamma - X$ transfer at heterointerfaces. The good agreement between experimental and theoretical results at low bias demonstrates that in our structure the $\Gamma - X$ transfer is more closely related to an elastic process involving an AlAs X-point longitudinal effective mass for tunneling electrons.

I. Introduction

$\Gamma - X$ intervalley tunneling in AlAs/GaAs structures has been a subject of great interest in Semiconductor Physics^[1-8]. Recently the $\Gamma - X$ intervalley tunneling has also been observed in heterostructures based on alternative AlSb/InAs materials^[9]. For the analysis of the $\Gamma - X$ electronic transfer in AlAs/GaAs single quantum barriers (SQB) considered in this work, two main processes must be taken into account: (i) tunneling electrons originating at the Γ -point GaAs emitter in the (100) direction can transfer elastically to a longitudinal AlAs X-point ellipsoid [lying along (100) axis] because the translational symmetry of the lattice is broken in the growth direction; (ii) Γ electrons can be transferred via inelastic scattering to a X-ellipsoid transverse to the (100) direction by phonons or inter-

face roughness. These intervalley tunneling processes involve, respectively, either the AlAs X-point longitudinal effective mass $m_{Xl} = 1.1m_0^{[10]}$, or the AlAs X-point transverse effective mass $m_{Xt} = 0.19m_0^{[10]}$ (m_0 is the free electron mass). The energy of the electronic states in the AlAs well formed by the X-conduction band minima (Fig. 1) would thus depend not only on the $\Gamma - X$ barrier ($\Delta E_{\Gamma X}$) but also on the kind of AlAs X-point effective mass involved. Because at resonances the energy of the Γ incident electrons coincides with the energy of the quantum levels in the X-well, new features related to the negative differential conductivity (NDC) regions in the I(V) curves are expected.

$\Gamma - X$ resonant tunneling effects in an AlAs/GaAs SQB under hydrostatic pressure were firstly investigated by Ohno, Mendez and Wang^[7]. They have observed a well defined NDC region in the I(V) curve at

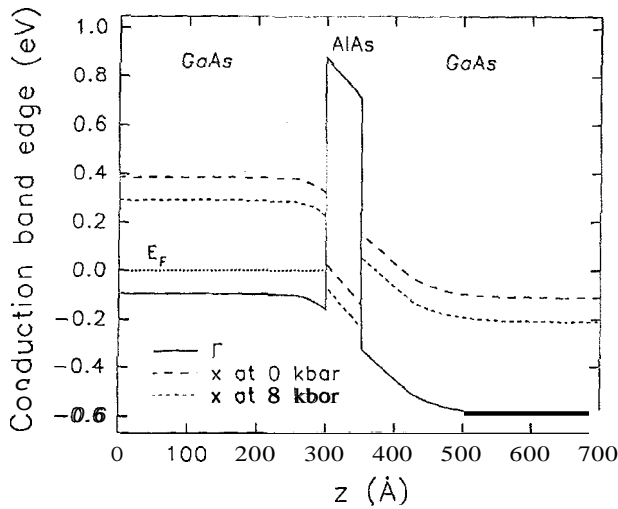


Figure 1: Single barrier structure scheme for the Γ (solid line) and X (dashed line, for two pressures) band-edge profiles at 0.5 V. The position of the Fermi level in the emitter is also shown.

77K. Their conclusion, supported by theoretical estimations is that the $\Gamma - X$ transfer is primarily controlled by an inelastic process involving a X-point transverse effective mass.

In this work, we report experimental and theoretical results on the basic process of the $\Gamma - X$ intervalley transfer of electrons tunneling through AlAs/GaAs SQB under hydrostatic pressure. Other measurements at atmospheric pressure and different temperatures are also presented. Two features appear in our $I(V)$ curves due to resonant tunneling involving $\Gamma - X$ intervalley transfer. The behaviour of the first feature at low bias is very well described by our calculations. However, a larger discrepancy between theory and experiment is observed for the feature at higher biases. This is attributed to the fact that charge accumulation in the X-well of the AlAs barrier is not taken into account in our calculations. The main mechanism for the $\Gamma - X$ resonant tunneling effect in our AlAs/GaAs SQB does not involve an inelastic process, as reported in Ref. 7. In our case it is more closely related to an elastic process which involves a heavier AlAs X-point longitudinal effective mass for tunneling electrons. Elastic processes were also recently reported for the $\Gamma - X$ intervalley tunneling of electrons in AlSb/InAs double barrier heterostructures^[9].

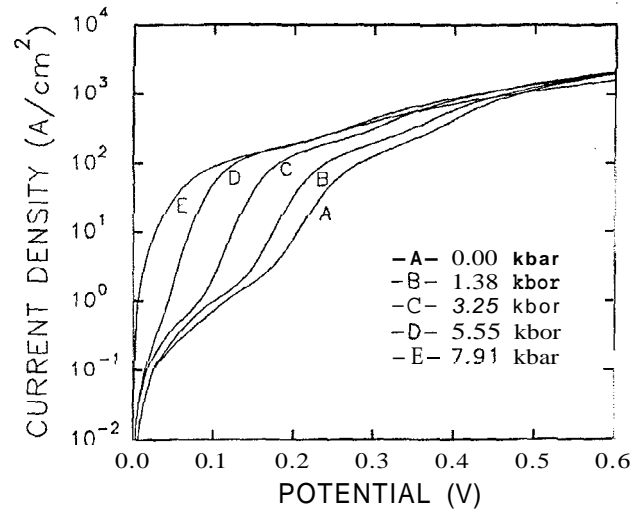


Figure 2: Experimental $I(V)$ curves obtained with a 5.2 nm barrier at 4.2K and for different applied pressures.

II. Results and discussions

Measurements were made in two sets of samples with an AlAs layer thickness of 5.2 nm and 4.1 nm, respectively. The structure of the samples consisted of (i) a n^+ -GaAs (Si doped $\sim 2 \times 10^{18} \text{ cm}^{-3}$) buffer layer $\sim 0.5 \mu\text{m}$ thick grown on (100) n^+ -GaAs substrates, (ii) a 5.0 nm thick undoped GaAs spacer layer, (iii) The undoped AlAs barrier, (iv) a 5.0 nm undoped spacer layer and (v) a n^+ -GaAs (Si doped $\sim 2 \times 10^{18} \text{ cm}^{-3}$) top contact layer $\sim 0.5 \mu\text{m}$ thick. The other growth details and lithography of the samples are described in Ref. 8.

The liquid clamp cell technique is used to produce hydrostatic pressure up to 9 kbar. Under pressure the X-band edge moves relatively to the Γ -band edge at a rate of $d(E_X - E_\Gamma)/dP = -12.07 \text{ meV/kbar}$ in GaAs^[11]. It is assumed the same rate for the AlAs Γ -band edge relative to the AlAs Γ -band edge. In Fig. 1 are shown the calculated band diagram of the SQB structure for pressures of 0 and 8.0 kbar and for an applied voltage of 0.5 V.

The measured and calculated $I(V)$ curves are shown in Figs. 2 and 3, respectively, for different applied pressures. The behaviour of these curves can be understood qualitatively. At low voltages the major part of current is attributed to the direct Γ electron tunneling. The

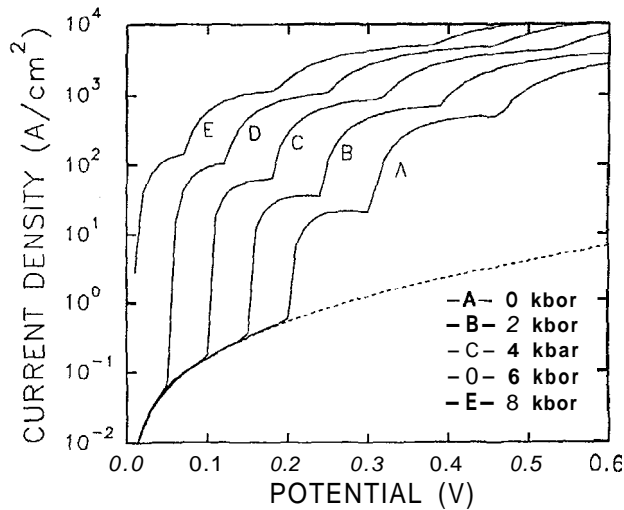


Figure 3: Calculated $I(V)$ curves at different pressures for a sample with a barrier thickness of 5.2 nm. The dashed line shows the contribution of the $\Gamma - \Gamma - \Gamma$ process to the tunneling current.

emitter Fermi level is still below the fundamental level of the X-band quantum well in the barrier. The X-component of the wave-function in this case, is attenuated more rapidly than the Γ -component due to the heavier X-point effective mass. When the Fermi level approaches a X-well quantum level, a rapid increase of current occurs because of $\Gamma - X$ resonant tunneling. The steplike features which appear after these increases of current correspond to crossover the Fermi level and the X-well quantum levels. Within the pressure range studied only two NDC regions were observed in the $I(V)$ curves (Fig. 2), less than predicted by theory (Fig. 3). The observed features are also weaker and broader than predicted theoretically.

In our calculations we used a model developed by Liu^[3,4] within the effective mass approximation. The $\Gamma - X$ intervalley transfer is assumed to occur at the interfaces, induced by an interaction potential in the form of a Delta-function of strength α . The band profile of the SQB structure is obtained at a given bias by solving numerically the Poisson equation in a Thomas-Fermi approximation. The charge density in the X-well of the AlAs barrier is also neglected. We took the $\Gamma - X$ barrier height as $\Delta E_{\Gamma X} = 0.35 \text{ eV}$ ^[10] and used an effective mass for the Γ electron in the GaAs

layers of $0.067 m_0$ at atmospheric pressure, with an increase of 0.8%/kbar. Other quantities involved in the model, assumed to be pressure independent, are the longitudinal effective mass of X electrons, $1.3 m_0$ in GaAs and $1.1 m_0$ in AlAs, AlAs Γ -band effective mass, taken as $0.103 m_0$, $\alpha = 0.155 \text{ eV-Å}$, and the AlAs Γ barrier height, 0.98 eV in our case^[10].

All incident electrons in the emitter GaAs layer are assumed to be in the Γ -valley. This assumption implies that electrons can tunnel through the whole SQB structure following three possible processes, namely $\Gamma - \Gamma - \Gamma$, $\Gamma - X - \Gamma$ or $\Gamma - X - X$. The $\Gamma - \Gamma - \Gamma$ process gives rise to the usual exponential behaviour in the $I(V)$ curves. The contribution of this process to the calculated current is shown in Fig. 3 by the dashed line. The dashed curve was obtained at 0 kbar by turning off the $\Gamma - X$ interaction at the interfaces (i.e., by putting $\alpha = 0$) while keeping the same values to other parameters. In the $\Gamma - X - \Gamma$ process, the current starts to increase each time the energy levels of the X-band quantum well approaches the Fermi level of the GaAs emitter layer. An important enhancement of the current is then obtained when the resonant tunneling effect through the X-valley takes place. Once the electrons are transferred to the X-valley, they will propagate through the AlAs barrier without substantial attenuation until they are transferred back to the Γ -valley of the GaAs collector layer. The contribution of the $\Gamma - X - \Gamma$ process was found to be much stronger than the $\Gamma - X - X$ process^[8] in all our conditions of pressure and bias. The $\Gamma - X - X$ process becomes important only at a bias voltage larger than 0.8 V at atmospheric pressure.

Since an increase of hydrostatic pressure shifts the X-profile down relatively to the Γ -one, the energy levels in the X-band quantum well are also shifted at a given applied voltage. At zero bias, these quantized levels get closer to the Fermi level of emitter when pressure increases, resulting in a smaller bias needed to reach $\Gamma - X$ resonant tunneling conditions. This explains why steplike features in Figs. 2 and 3 are shifted to

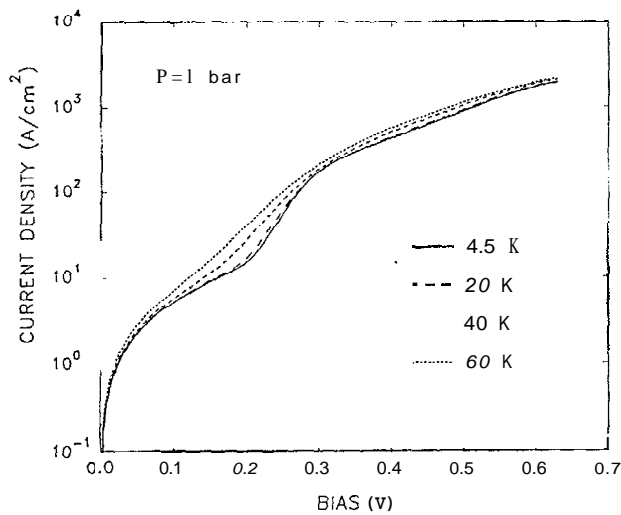


Figure 4: Experimental $I(V)$ curves obtained with a 4.1 nm barrier at atmospheric pressure and for different temperatures.

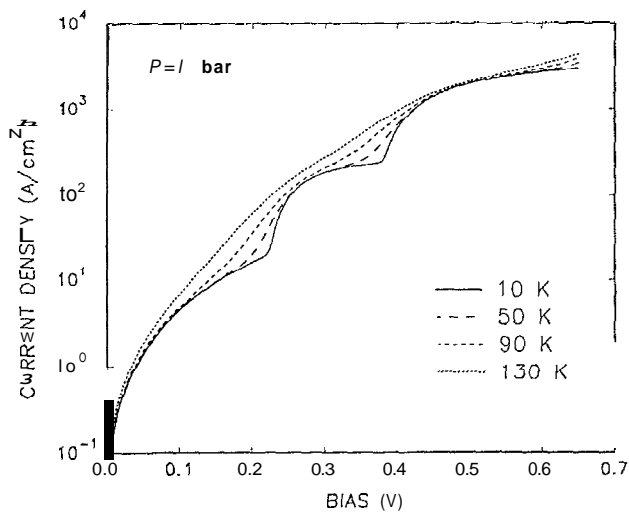


Figure 5: Calculated $I(V)$ curves for different temperatures at atmospheric pressure for a sample with a barrier thickness of 4.1 nm.

lower voltage as hydrostatic pressure increases

The experimental and theoretical results for the $I(V)$ curves at different temperatures are shown, respectively, in Figs. 4 and 5 for a barrier layer thickness of 4.1 nm. The increase of the temperature from 4.2 K to 120 K (Fig. 4) results in a progressive weakening of the NDC regions in the $I(V)$ curves in agreement with our theoretical results (Fig. 5). The weakening of the NDC regions by increasing temperature may be probably explained by the thermic excitation which increases the number of incident electrons tunneling the structure through the $\Gamma-\Gamma-\Gamma$ channel. This would lead to an en-

hancement of the exponential contribution to the $I(V)$ characteristics, which might mask the contribution of the $\Gamma-X-\Gamma$ process, specially at higher biases.

The theoretical curves shown in Figs. 3 and 5 were obtained by considering only an elastic process, whereby the transfer occurs at the longitudinal X-valley, i.e., parallel to the growth direction (100). The agreement between theory and experiment, in all pressure and temperature ranges considered, demonstrates that, in our samples, the tunneling via $\Gamma-X-\Gamma$ process involving the longitudinal X-valley is the major cause for the NDC structures observed in the $I(V)$ characteristics. The transfer to the transverse X-valley would require a smaller effective mass $m_{X\perp} = 0.19 m_0$, leading to a higher confinement energy in the X-band quantum well and, correspondingly, to higher onset voltages for the NDC structures appearing in the $I(V)$ curves. The application of an electric field further increases this upward shift of the quantized levels relatively to the bottom of the well, which is more noticeable for smaller effective masses. In addition, our calculations using the X-point transverse effective mass reveals only a single structure in the theoretical $I(V)$ curve (not shown) at 0.23 V and at atmospheric pressure for our 5.2 nm barrier thickness sample, whereas experimentally there are two NDC structures.

In Figs. 6 and 7, the voltage position of the first two steplike features in the $\log(J)$ vs V curves is shown as a function of pressure at 4.2 K and as function of temperature at atmospheric pressure, respectively. These positions were determined by the voltages at which peaks occur in the first derivative ($d[\log(J)]/dV$ vs V) for both experimental and calculated curves, respectively. For the NDC structure appearing at lower voltage [for pressure and temperature studies (Figs. 6 and 7)], the agreement between experimental and theory is very good, whereas the second NDC structure appears experimentally at a voltage higher than predicted by theory. The discrepancy between theory and experiments at larger biases is probably due to the charge

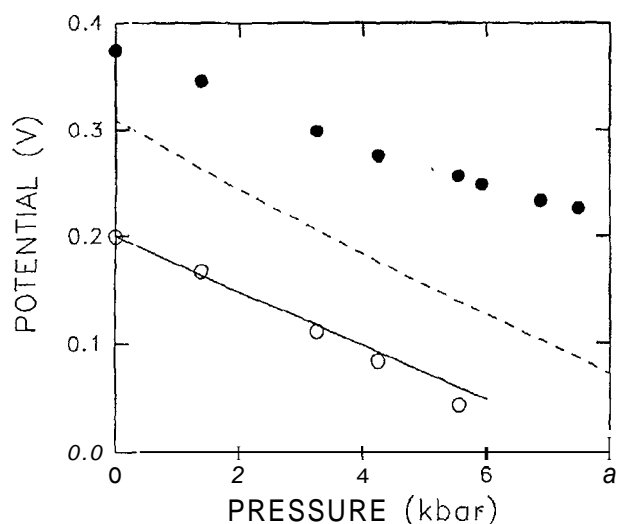


Figure 6: Position of the first two steplike features in the $I(V)$ curves, as a function of pressure, for the 5.2 nm barrier thickness sample. Open and solid dots correspond to experimental results (Fig. 2); Solid and dashed lines were obtained from the theoretical results (Fig. 3). The values were determined by finding the peak position in the first derivative of the experimental and theoretical $\log(J)$ vs. V curves.

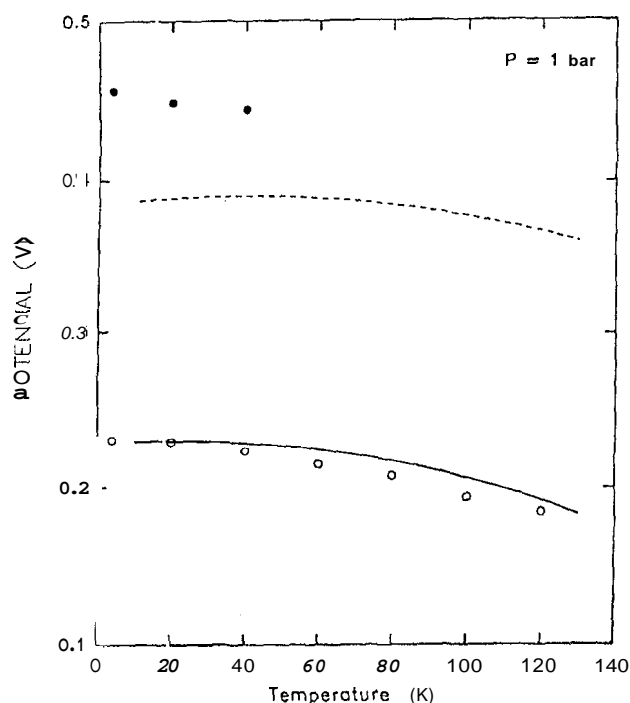


Figure 7: Position of the first two steplike features in the $I(V)$ curves, as a function of temperature, for the 4.1 nm barrier thickness sample. Open and solid dots correspond to experimental results (Fig. 4); Solid and dashed lines were obtained from the theoretical results (Fig. 5). The values were determined by the same procedure as described in the caption of Fig. 3.

accumulation in the AlAs X-band. Since the X-band quantum well is formed in the AlAs layer, one can expect that the electrons transferred to the longitudinal X-valley have a relatively long dwell time in this region. This will give rise to a charge accumulation and consequently to a band bending in the well that will push the quantized levels to higher energies producing the second resonance condition at corresponding higher voltages. Furthermore, one can also attribute the fact that the resonances associated with higher energy levels are not observed experimentally at the voltage positions predicted by our model to the lack of taking a proper account of charge accumulation in the calculations.

The elastic or inelastic character of the $\Gamma - X$ intervalley transfer is strongly dependent on the roughness degree of the interfaces present in the samples, what may explain the discrepancies between our observations and interpretation and those of Ref. 7.

III. Conclusions

$I(V)$ measurements under hydrostatic pressure at 4.2K and for different temperatures at atmospheric pressure were made on AlAs single quantum barriers. For both studies the results obtained at low bias, concerning the contribution of $\Gamma - X - \Gamma$ process to the tunneling current, are in good agreement with our theoretical predictions which consider elastic process involving the transfer of Γ electrons through the longitudinal X-valley in the AlAs barrier. The discrepancy between our experimental and calculated results at higher biases is probably due to the charge accumulation in the X-band quantum well, not considered by our theory.

References

1. E. E. Mendez, W. I. Wang, E. Calleja and C. E. T. Goniçalves da Silva, *Appl. Phys. Lett.* 50, 1263 (1987).
2. K. V. Rousseau, K. L. Wang and J. N. Schulman, *Appl. Phys. Lett.* 54, 1341 (1989).

3. H. C. Liu, *Appl. Phys. Lett.* **51**, 1019 (1987).
4. H. C. Liu, *Superlatt. Microstruct.* **7**, 35 (1990).
5. D. Landheer, H. C. Liu, M. Buchanan and R. Stoner, *Appl. Phys. Lett.* **54**, 1784 (1980).
6. A. C. Marsh, *Semicond. Sci. Technol.* **1**, 320 (1986).
7. H. Ohno, E. E. Mendez and W. I. Wang, *Appl. Phys. Lett.* **56**, 1793 (1990).
8. Y. Carbonneau, J. Beerens, L. A. Cury, H. C. Liu and A. S. Buchanan, *Appl. Phys. Lett.* **62**, 1955 (1993).
9. R. E. Carnahan, M. A. Maldonado, K. P. Martin, A. Nogaret, R. J. Higgins, L. A. Cury, D. K. Maude, J. C. Portal, J. F. Chen and A. Y. Cho, *Appl. Phys. Lett.* **62**, 1385 (1993).
10. S. Adachi, *J. Appl. Phys.* **58**, R1 (1985).
11. D. J. Wolford and J. A. Bradley, *Solid State Commun.* **53**, 1069 (1985).
12. L. G. Shantarama, A. R. Adams, C. N. Ahmad and R. J. Nicholas, *J. Phys. C* **17**, 4429 (1984).